JOURNAL OF AGRICULTURAL AND FOOD CHEMISTRY

Article

pubs.acs.org/JAFC

Antioxidant Activities of Curcumin and Ascorbyl Dipalmitate Nanoparticles and Their Activities after Incorporation into Cellulose-Based Packaging Films

Piyapong Sonkaew, Amporn Sane, and Panuwat Suppakul*

Department of Packaging and Materials Technology, Faculty of Agro-Industry, and Center for Advanced Studies in Nanotechnology for Chemical, Food and Agricultural Industries, Kasetsart University, 50 Phaholyothin Road, Chatuchak, Bangkok 10900, Thailand

ABSTRACT: Curcumin (Ccm) and ascorbyl dipalmitate (ADP) nanoparticles (NPs) with average sizes of ~50 and ~80 nm, respectively, were successfully produced by rapid expansion of subcritical solutions into liquid solvents (RESOLV). Pluronic F127 was employed as a stabilizer for both Ccm- and ADP-NPs in an aqueous receiving solution. Antioxidant activities of the Ccm-NPs and ADP-NPs were subsequently investigated using four assays, including 2,2-diphenyl-1-picrylhydrazyl (DPPH) radical scavenging, ABTS radical cation decolorization, β-carotene bleaching, and ferric reducing antioxidant power. Ccm-NPs and ADP-NPs showed higher antioxidant activities than those of Ccm and ADP. Ccm-NPs yielded higher antioxidant activities than those of Ccm in ethanol and water (Ccm-EtOH and Ccm-H_2O), respectively. ADP-NPs yielded lower antioxidant activities than that of ADP in ethanol (ADP-EtOH) but higher activities than that of ADP in water (ADP-H_2O). Moreover, incorporation of Ccm-NPs and ADP-NPs into cellulose-based films indicated that Ccm-NPs and ADP-NPs significantly enhanced the antioxidant activities of Ccm and ADP ($p < 0.05$). Our results show that the environmentally benign supercritical CO_2 technique should be generally applicable to NP fabrication of other important bioactive ingredients, especially in liquid form. In addition, we suggest that Ccm-NPs and ADP-NPs can be used to reduce the dosage of Ccm and ADP and improve their bioavailability, and thus merit further investigation for antioxidant packaging film and coating applications.

KEYWORDS: *antioxidant activity, antioxidant packaging, ascorbyl dipalmitate, biopolymer, cellulose-based packaging film, curcumin*

INTRODUCTION

The sensory quality of a food is one of the major determinants of its appeal to consumers and, consequently, sales of the product. Lipid oxidation is one of the main factors affecting food quality loss and shelf life reduction. Therefore, delaying lipid oxidation is highly relevant to the food industry. Oxidative processes in food products lead to the degradation of lipids and proteins, resulting in the deterioration in flavor, texture, and color of the products.[1] It is a paradox of aerobic life that aerobic organisms require oxygen for their normal metabolisms, yet oxygen can be toxic to cellular material.[2] Detrimental events which may be caused by lipid oxidation include membrane fragmentation, disruption of membrane-bound enzyme activity, swelling and disintegration of mitochondria, and lysosomal lysis.

Since the oxidative deterioration of fat components in food products is responsible for off-flavors and rancidity, which decrease nutritional and sensory qualities, the addition of antioxidants is required to preserve product quality. Synthetic antioxidants, for example, butylated hydroxytoluene (BHT), butylated hydroxyanisole (BHA), *tert*-butylhydroquinone (TBHQ), and propyl gallate (PG), are widely used as antioxidants in the food industry. Their safety, however, has been questioned.[3] BHA was revealed to be carcinogenic in animal experiments. At high doses, BHT may cause internal and external hemorrhaging, which leads to death in some strains of mice and guinea pigs.[4] In recent years there has been increasing interest among food manufacturers in the use of natural antioxidants, to act as replacements for currently used synthetic antioxidants.[5]

As a principal curcuminoid, curcumin (Ccm) (Figure 1) is a phenolic compound derived from the root of turmeric (*Curcuma longa* L.). This compound has been employed for hundreds of years in Asian countries as a food additive to enhance flavor and color.[6] It is also currently used in the pharmacological and food industries.[7] Curcumin possesses powerful antioxidant properties and hence has recently attracted much attention owing to its crucial bioactive potential. Ascorbyl dipalmitate (ADP) (Figure 1) is a fatty ester derivative of ascorbic acid; it is poorly soluble in water and does not spontaneously form micelles or liposomal structures in water. ADP has been extensively used as an additive to prevent oxidation in foods, pharmaceuticals, and cosmetics.[8]

Apart from such bioactive compounds, recent innovations in nanotechnology offer great promise in fulfilling the broad functional requirements of oxidation prevention. Nanoparticles (NPs) could be coupled with active packaging to potentially allow the use of smaller dosages of bioactive compounds, together with an increase in surface area, enhancement of solubility, and an increase in bioactivity of active substances.[9−13] Rapid expansion of subcritical solutions into liquid solvents (RESOLV), which has been developed based on supercritical fluid technology, is a versatile technique for producing stable suspensions of well-dispersed and uniform nanoparticles.[14−16] In this process, a subcritical

Received: March 27, 2012
Revised: May 10, 2012
Accepted: May 14, 2012
Published: May 14, 2012

dx.doi.org/10.1021/jf301311g | J. Agric. Food Chem. 2012, 60, 5388−5399

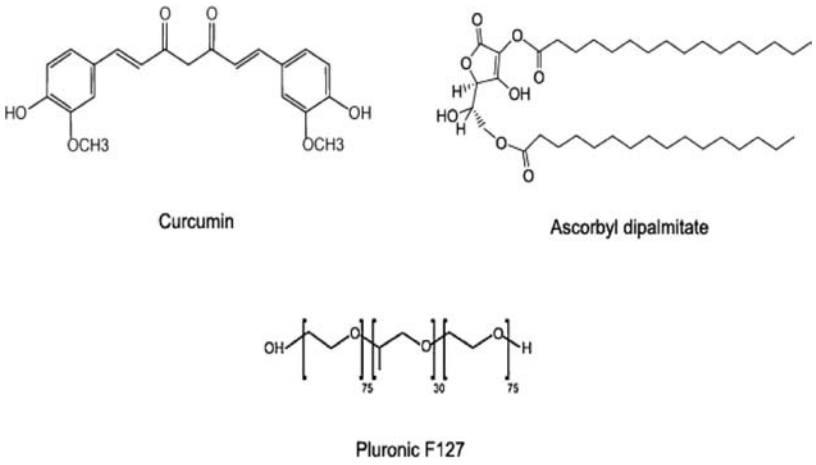

Figure 1. Chemical structures of curcumin, ascorbyl dipalmitate, and Pluronic F127.

solution containing a solute and a solvent is directly expanded across a nozzle into a liquid receiving solution. This method is capable of producing nanoparticles from a variety of compounds because a polar organic cosolvent (or modifier) can be added to supercritical carbon dioxide in order to dissolve the solutes at moderate pressures.

Cellulose is the most abundant organic renewable resource in the plant kingdom. It is a polysaccharide composed of linear chains of (1−4)-β-D-glucopyranosyl units. Cellulose derivatives (e.g., methylcellulose, hydroxypropyl cellulose, hydroxypropyl methylcellulose, carboxymethyl cellulose, and microcrystalline cellulose) have unique physical, chemical, and colloidal properties, and an ability to form films. Accordingly, they have been used as edible films and coatings since the 1980s.[17]

Antioxidant (AO) packaging technology, an innovative concept, can be defined as a version of active packaging (AP) in which the package, the product, and the environment interact to limit or prevent lipid oxidation by donating electrons or hydrogen, quenching oxygen, and/or scavenging free radicals. By this action, the shelf life of the product is prolonged and its quality and safety are better preserved.[18] Because of the perceived lower risk to the consumer, the use of naturally derived AO additives (e.g., plant extracts and plant volatile components) is of increasing interest.[19] As no single AO additive can cover all the needs for food preservation, it is important to investigate different kinds of potential compounds in order for this technology to become successful.

Numerous packaging films have been investigated for their antioxidant properties. Wessling et al.[20] reported the antioxidant ability of low-density polyethylene (LDPE) film impregnated with either 3,5-di-*tert*-butyl-4-hydroxytoluene (BHT) or α-tocopherol (vitamin E). Lee et al.[21] reported the antioxidant activity of high-density polyethylene (HDPE) coextruded with ethylene vinyl acetate (EVA) film incorporated with BHT or vitamin E. Jongjareonrak et al.[22] reported the antioxidative properties of fish skin gelatin films incorporated with BHT or vitamin E. Siripatrawan and Harte[23] reported the antioxidant activity of chitosan film incorporated with green tea extract. Recently, Bao et al.[24] reported that gelatin films incorporated with tea polyphenol-loaded chitosan nanoparticles possessed antioxidant properties. However, there is still only limited information on the utilization of curcumin and ADP as antioxidants to be incorporated into packaging films and coatings. Hence, it is very important to investigate the possibility of producing antioxidant packaging film by the incorporation of curcumin nanoparticles.

The present study was aimed at (1) preparing curcumin and ascorbyl dipalmitate nanoparticles (Ccm-NPs and ADP-NPs) using the RESOLV process; (2) investigating the antioxidant activities of Ccm-NPs and ADP-NPs; and (3) investigating the antioxidant activities of cellulose-based packaging films containing Ccm-NPs and ADP-NPs.

MATERIALS AND METHODS

Materials. Curcumin, L-ascorbyl 2,6-dipalmitate, Trolox (6-hydroxy-2,5,7,8-tetramethychroman-2-carboxylic acid), and 2,2-diphenyl-1-picrylhydrazyl (DPPH) were purchased from Sigma-Aldrich (Steinheim, Germany). Iron(III) chloride hexahydrate and β-carotene were purchased from Fluka (Buchs, Switzerland). Pluronic F127 (Figure 1), 2,2′-Azobis(2-methylpropionamidine) dihydrochloride, 3-*tert*-butyl-4-hydroxyanisole (BHA), 3,5-di-*tert*-butyl-4-hydroxytoluene (BHT), 2,2′-azino-bis(3-ethylbenzothiazoline-6-sulfonic acid) (ABTS), Tween 40 (polyoxyethylene sorbitan monopalmitate), and sodium acetate trihydrate were obtained from Sigma-Aldrich (St. Louis MO, USA). Ethanol was supplied by the Liquor Distillery Organization, Excise Department, Ministry of Finance (Chachoengsao, Thailand).

Ccm-NPs and ADP-NPs Preparation. To prepare Ccm-NPs and ADP-NPs, RESOLV experiments were carried out by expanding subcritical solutions of Ccm and ADP in mixtures of ethanol and supercritical CO_2 (1:1 w/w) across a nozzle (50 μm dia., L/D = 4) into a receiving solution (Figure 2). The details of the rapid expansion

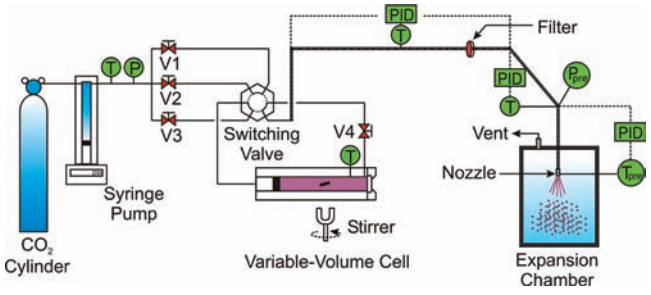

Figure 2. Schematic of RESOLV apparatus.

apparatus setup have been described in our previous reports.[15,16] Briefly, the variable-volume cell was charged with 0.097 g of a solute (Ccm or ADP), 16.1 g of ethanol, and 16.1 g of CO_2. The mixture was then pressurized to 173 bar, heated to 45−50 °C, and continuously stirred until a homogeneous solution was obtained. Next, pure CO_2 was allowed to flow from the syringe pump, bypassing the high-pressure

dx.doi.org/10.1021/jf301311g | J. Agric. Food Chem. 2012, 60, 5388−5399

cell, and subsequently expand across the nozzle in order to establish steady-state conditions with a pre-expansion temperature (T_{pre}), measured upstream of the nozzle, of 80 °C (Figure 2). Then the flow of CO_2 was rapidly diverted to the view cell, indirectly pushing the subcritical solution out of the cell by means of a movable piston. The solution was subsequently expanded through the nozzle into 50 mL of 0.1 wt % F127 aqueous solution or 3 wt % methyl cellulose solution by submerging the nozzle 1 cm below the liquid surface.

In Vitro Quantification of Ccm-NPs and ADP-NPs. For in vitro quantification of Ccm-NPs and ADP-NPs in both 0.1 wt % F127 aqueous solution and 3 wt % methyl cellulose solution, the procedure was slightly modified in accordance with a recent report.[25] A standard solution of either Ccm or ADP in ethanol was prepared by dissolving 2 mg of substance in 20 mL of 95% ethanol solution. The assay system used a UV-2450 UV−vis spectrophotometer (Shimadzu, Tokyo, Japan) at 190−600 nm for determining λ_{max} of substances. To obtain an absorbance standard curve of Ccm, serial dilutions from 2 to 8 μg mL^{-1} of Ccm in ethanol were analyzed, at a maximum wavelength of 427 nm in an absorbance range of 0.3−1.8, R^2 = 0.9957. For ADP standard, serial dilutions from 20−80 μg mL^{-1} were determined at a maximum wavelength of 254 nm in an absorbance range 0.5−1.1, R^2 = 0.9958. The data were plotted in a straight line for the quantification of unknown samples in a nanoparticle suspension.

Particle Size and Morphological Characterization. Aqueous suspensions of Ccm and ADP particles obtained from RESOLV experiments were characterized by the dynamic light scattering (DLS) method, using a Zetasizer Nano ZS90 (Malvern Instruments, Malvern, UK) to measure the hydrodynamic diameter (d_h) of Ccm and ADP particles.[26,27]

The particle size and morphology of Ccm and ADP were also characterized by transmission electron microscopy (TEM) using a Hitachi model H-7650 (Hitachi, Tokyo, Japan) with an accelerating voltage of 100 kV. Samples were prepared by depositing ∼100 μL of the RESOLV suspension onto a copper grid and then drying under a vacuum (1 bar) at ambient temperature for 1 week. Particle sizes were determined using Image-Pro Plus version 6.0 software.[14]

Ccm-NPs and ADP-NPs Solution Preparation. To prepare the control solutions of either Ccm or ADP in water (Ccm-H_2O or ADP-H_2O), according to a recently reported procedure,[28] 93 mg of substance was added to 100 mL of distilled water and then placed in a supersonic water bath for 10 min. Subsequently, the suspension was centrifuged at 1000 rpm for 10 min, and the supernatant was used as stock solution of either Ccm-H_2O or ADP-H_2O. For the preparation of BHA, BHT, Ccm in ethanol (Ccm-EtOH) and ADP in ethanol (ADP-EtOH), 10 mg of substance was dissolved with 100 mL of 40% ethanol and directly used as the stock solution of the substance.

Determination of DPPH Radical Scavenging Activity. Free radical scavenging activity of selected substances was determined according to a previously reported procedure, using the stable DPPH radical[7,29] with some modifications. One milliliter of selected substances in 0.1 wt % F127 solution (BHA, BHT, ADP-EtOH, ADP-H_2O, ADP-NPs, Ccm-EtOH, Ccm-H_2O, and Ccm-NPs) was added to 0.5 mL of solution containing 0.1 mM of DPPH radical in 0.1 wt % F127 solution at different concentrations. The solutions were vortexed thoroughly and allowed to react for 30 min in the dark. All experiments were performed in triplicate. Absorbance of the solution was measured at 517 nm. The percentage of free radical scavenging was calculated according to eq 1 as a percentage of DPPH scavenging. The sample concentration providing 50% of radical scavenging activity (EC_{50}) was calculated from the graph of DPPH scavenging percentage against sample concentration.

$$\text{DPPH radical scavenging (\%)} = \left[1 - \frac{\text{absorbance of sample}}{\text{absorbance of control}}\right] \times 100 \quad (1)$$

Determination of ABTS Radical Cation Scavenging Activity. ABTS also forms a relatively stable free radical, which decolorizes in its nonradical form. Spectrophotometric analysis of ABTS radical cation scavenging activity was determined by a modified method of Ak and Gülçin.[7] In this procedure, ABTS radical cations were produced by reacting 2 mM ABTS in H_2O with 2.45 mM potassium persulfate ($K_2S_2O_8$), and then storing in the dark at room temperature for 16 h. The ABTS radical cation solution was diluted to give an absorbance at 734 nm in 0.1 wt % F127 solution. Then, 600 μL of ABTS radical cation solution was added to 600 μL of each sample solution (BHA, BHT, ADP-EtOH, ADP-H_2O, ADP-NPs, Ccm-EtOH, Ccm-H_2O, and Ccm-NPs) in 0.1 wt % F127 solution at different concentrations. The absorbance was recorded 30 min after mixing, and the percentage of radical scavenging was calculated for each concentration relative to a blank solution containing no scavenger. The sample concentration providing 50% of radical scavenging activity (EC_{50}) was calculated from the graph of ABTS radical cation scavenging percentage against sample concentration.

$$\text{ABTS radical cation scavenging(\%)} = \left[1 - \frac{\text{absorbance of sample}}{\text{absorbance of control}}\right] \times 100 \quad (2)$$

Determination of β-Carotene Linoleate Oxidative Bleaching. Antioxidant activity was investigated using a β-carotene linoleate oxidative bleaching technique.[30,31] β-Carotene (0.2 mg) in 0.2 mL of chloroform was mixed with linoleic acid (20 mg) and Tween 40 (200 mg). Chloroform was removed at 40 °C under a vacuum, and the resulting mixture was diluted with 10 mL of water and mixed well. To this emulsion, 40 mL of oxygenated water was added. Then 4 mL aliquots of the mixed emulsion were pipetted into test tubes containing 0.5 mL of 100 μg mL^{-1} of the different substances. A control containing 0.5 mL of 0.1 wt % F127 solution and 4 mL of the above emulsion was prepared. The tubes were placed in a water bath at 50 °C. The absorbance at 470 nm was taken at zero time (t = 0) and at the time of color disappearance in the control tubes (t = 180 min). A mixture prepared as above without β-carotene served as a blank. All determinations were carried out in triplicate. Antioxidant activity was evaluated in terms of oxidative bleaching of β-carotene linoleate using the following formula:

$$\%AA = \left[\frac{Ae(180) - Ac(180)}{Ac(0) - Ac(180)}\right] \times 100 \quad (3)$$

where $Ac_{(0)}$, $Ae_{(180)}$, and $Ac_{(180)}$ are the absorbance measured at zero time of the incubation for the control, and the absorbance measured in the test sample and the control, respectively, after incubation for 180 min.

Determination of Ferric Reducing Antioxidant Power. Ferric reducing antioxidant power (FRAP) assay was carried out by the method of Benzie and Strain[32] and Thaipong et al.[33] with minor modifications. The method is based on the reduction of a ferric 2,4,6-tripyridyl-*s*-triazine complex (Fe^{3+}-TPTZ) to the ferrous form (Fe^{2+}-TPTZ). The stock solutions included 300 mM acetate buffer (3.1 g of $C_2H_3NaO_2{\cdot}3H_2O$ and 16 mL of $C_2H_4O_2$) of pH 3.6; 10 mM TPTZ (2,4,6-tripyridyl-*s*-triazine) solution in 40 mM HCl; and 20 mM $FeCl_3.6H_2O$ solution. Fresh working solution was prepared by mixing acetate buffer, TPTZ solution, and $FeCl_3{\cdot}6H_2O$ solution in a 10:1:1 ratio, and then allowing the reaction at 37 °C before use. BHA, BHT, ADP-EtOH, ADP-H_2O, ADP-NPs, Ccm-EtOH, Ccm-H_2O, and Ccm-NPs (with a volume of 150 μL at a concentration of 100 μg mL^{-1}) were added to 3000 μL of fresh working solution and allowed to react for 30 min in the dark. The increase in absorbance at 593 nm was measured. The standard curve of Trolox was linear, in a range of 25−800 μM mL^{-1}. The results were expressed as Trolox equivalents (μM mL^{-1}).

Antioxidant-Incorporated Cellulose-Based Packaging Film Preparation. Cellulose ether solution was prepared by dissolving 10 g of methyl cellulose (Methocel Premium EP; Dow Chemical, Midland MI, USA) in 300 mL of distilled water. Three grams of polyethylene glycol 400 (Carbowax; Union Carbide, Houston TX, USA) was added to the above solution as a plasticizer to prevent brittleness. The solution was heated on a hot plate to 65 °C while stirring. Selected substance solutions (BHA, BHT, ADP-EtOH, ADP-H_2O, Ccm-EtOH,

and Ccm-H_2O) were then added to cellulose ether solution to obtain various concentrations of 0.1, 0.3, and 0.5 wt %. Moreover, ADP-NPs and Ccm-NPs, which were prepared by the RESOLV process by submergence in 3 wt % methyl cellulose solution, were also added to cellulose ether solution to obtain the same concentrations. The resulting solutions were degassed in an ultrasonic water bath (model 275D; Crest Ultrasonics, Trenton NJ, USA) for 10 min. Antioxidant film (30 mL) was cast on a glass plate, with linear low-density polyethylene (LLDPE) for substrate film, using a film coater (model PI-1210; Tester Sangyo, Saitama, Japan). The applicator speed for casting was set at 0.5 cm s^{-1}. The films were dried at room temperature for 24 h.

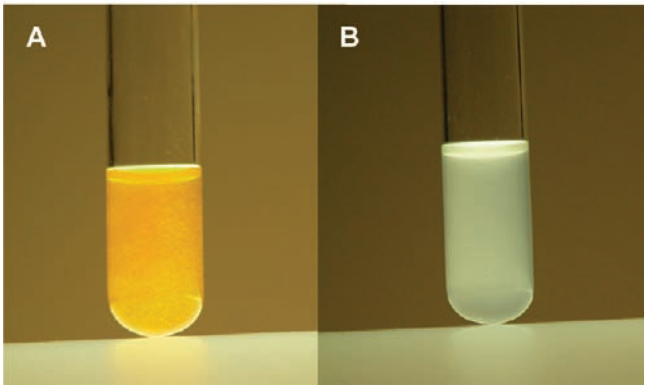

Figure 3. Nanoparticles obtained from RESOLV with T_{pre} = 80 °C and 330 bar in aqueous receiving solutions containing 0.1 wt % Pluronic F127 of curcumin (A) and ascorbyl dipalmitate (B).

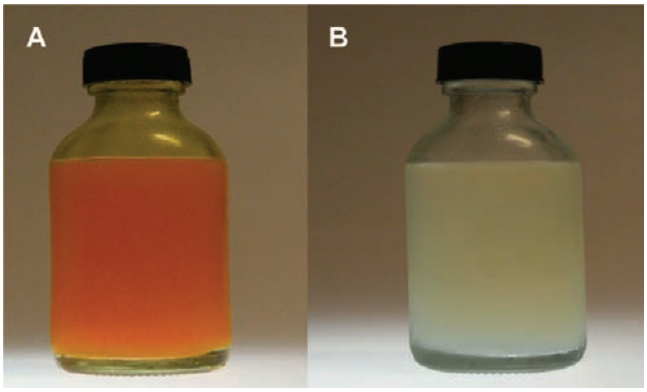

Figure 4. Nanoparticles obtained from RESOLV with T_{pre} = 80 °C and 330 bar in aqueous receiving solutions containing curcumin (A) and ascorbyl dipalmitate (B) in methyl cellulose solutions.

Film Characterization. *Film Thickness Measurement.* Film thickness was measured at five random positions around the film, using a model 7326 digital micrometer (Mitutoyo Manufacturing, Tokyo, Japan).

UV–vis Spectrophotometry. UV–vis spectrophotometry technique was performed according to the method of Siripatrawan and Harte[23] with some modification. Film absorbance was measured at 190–600 nm using a UV–vis spectrophotometer. The films were cut into rectangular pieces and placed directly in the spectrophotometer test cell. Methyl cellulose film was used as the reference. The UV–visible light of film at λ_{max} was calculated by the following equation:

$$T = \frac{\text{Abs of sample at } \lambda\text{max}}{x} \quad (4)$$

where T is the proportion of UV–visible light absorbance of films at λ_{max}, and x is the film thickness (mm). According to this equation, a high value of T indicates higher quantities of sample in the film.

Scanning Electron Microscopy (SEM). A JSM-6301F scanning electron microscope (JEOL, Tokyo, Japan) was used to study the morphology of nanoparticles and films. The samples were deposited onto aluminum specimen stubs using double-stick carbon tabs, and then coated with gold. All samples were examined using an accelerating beam at a voltage of 5 kV. Magnification of 10000× was used.

FTIR Analysis. Fourier transform infrared (FTIR) spectra of Ccm, ADP, methyl cellulose, and LDPE and FTIR spectra of Ccm-EtOH-, Ccm-H_2O-, Ccm-NPs-, ADP-EtOH-, ADP-H_2O-, and ADP-NPs-incorporated methyl cellulose-coated LDPE films were taken with a Bruker Tensor 27 FTIR spectrometer (Bruker, Karlsruhe, Germany) over a range of 4000 to 600 cm^{-1} in ATR mode. The FTIR spectra were used to determine the existence of functional groups of ADP and Ccm in methyl cellulose films.

Determination of Antioxidant Activities of the Films. *DPPH Radical Scavenging Assay.* Free radical scavenging activity was determined as described by Siripatrawan and Harte[23] with slight modifications. A 6 cm^2 sample of antioxidant film was dissolved in 6 mL of solution containing 0.1 wt % F127. One milliliter of film extract solution was mixed with 0.5 mL of DPPH radical (0.1 mM) in 40% ethanol and allowed to react for 30 min in the dark. All experiments were performed in triplicate.

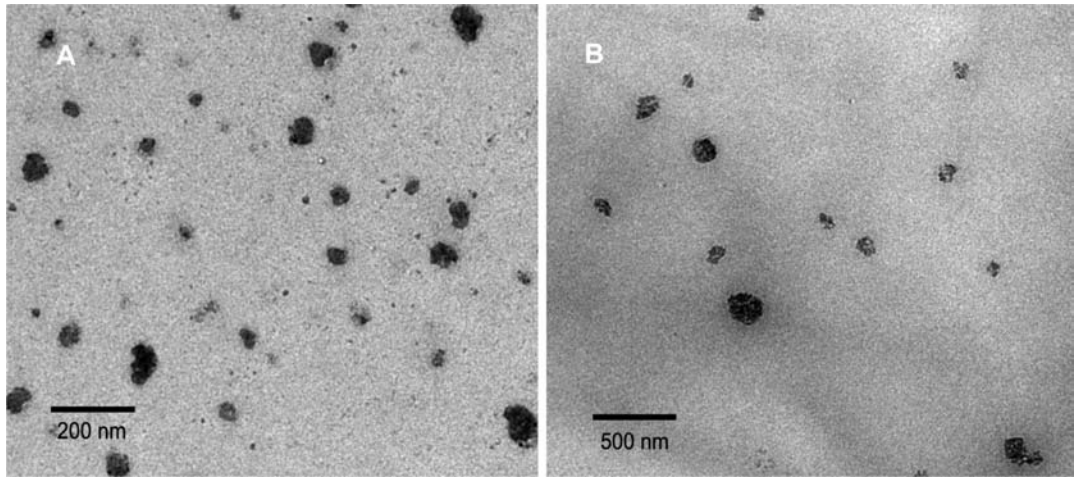

Figure 5. TEM images of nanoparticles at 12000× on a copper grid obtained from RESOLV with T_{pre} = 80 °C and 330 bar in aqueous receiving solutions containing 0.1 wt % Pluronic F127: Ccm-NPs (A) and ADP-NPs (B).

ABTS Radical Cation Scavenging Assay. Spectrophotometric analysis of ABTS radical cation scavenging activity was determined as described in the previous section. A 6 cm^2 sample of antioxidant film was dissolved in 6 mL of solution containing 0.1 wt % F127. One milliliter of film extract solution was mixed with 2 mM of ABTS radical cation solution in 0.1 wt % F127 and allowed to react for 30 min in the dark. All experiments were performed in triplicate.

β-Carotene Linoleate Oxidative Bleaching Assay. Antioxidant activity was investigated using a β-carotene linoleate oxidative bleaching technique, as described in the previous section. A 4 cm^2 sample of antioxidant film was dissolved in 4 mL of solution containing 0.1 wt % F127. Then 0.5 mL of film extract solution was added to 4 mL of solution containing aliquots of the emulsion. All experiments were performed in triplicate.

Ferric Reducing Antioxidant Power Assay. FRAP assay was performed as described in the previous section. A 3 cm^2 sample of antioxidant film was dissolved in 3 mL of solution containing 0.1 wt % F127. One milliliter of film extract solution was added to 3 mL of ferric reagent and allowed to react for 30 min in the dark.

Data Analysis. A completely randomized design (CRD) was used as an experimental design. Experimental data were subjected to one-way analysis of variance (ANOVA) using the SPSS 16.0 for Windows (SPSS Inc., Chicago, IL, USA). The statistical significance of differences between mean values was established at $p \leq 0.05$; Duncan's new multiple range test was applied for all statistical analysis.

Table 1. Particle Sizes Obtained from DLS and TEM Measurements of Ccm-NPs and ADP-NPs Prepared by RESOLV of 0.3 wt % Ccm or ADP Solutions with T_{pre} = 80 °C and 173 bar into Aqueous Receiving Solutions Containing 0.1 wt % Pluronic F127

	DLS		TEM	
antioxidants	d_h range (nm)	$\overline{d_h}$ (nm)	d_h range (nm)	$\overline{d_h}$ (nm)
Ccm-NPs	44−80	43	26−93	53
	220−712	425		
ADP-NPs	91−165	125	32−160	77
	225−825	492		
	4145−5560	4835		

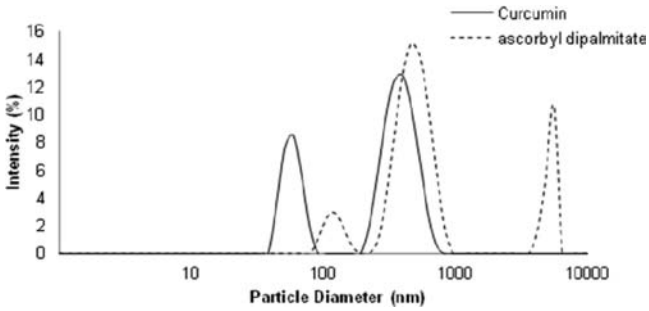

Figure 6. Particle size distributions of Ccm-NPs and ADP-NPs stabilized in 0.1 wt % Pluronic F127.

Table 2. Concentrations of Ccm-NPs and ADP-NPs in 0.1 wt % Pluronic F127 and 3 wt % Methyl Cellulose Solutions

	concentration ($mg \cdot mL^{-1}$)	
antioxidants	Pluronic F127 system	methyl cellulose system
Ccm-NPs	0.811 ± 0.04	1.14 ± 0.01
ADP-NPs	0.663 ± 0.02	2.10 ± 0.08

RESULTS AND DISCUSSION

Ccm and ADP Nanoparticles. Ccm-NPs and ADP-NPs stabilized in 0.1% F127 solutions and 3 wt % methyl cellulose solutions were produced by rapid expansion of 0.3 wt % Ccm and ADP subcritical solutions with pre-expansion pressure and temperature of 173 bar and 80 °C, respectively (Figures 3 and 4). As shown in Figure 5, the primary nanoparticles were strongly individual particles. Nevertheless, there was evidence that they slightly yielded apparent agglomeration (figure not shown). According to Jiang et al.,[34] it was found that probe ultrasonication performed better than bath ultasonication in dispersing TiO_2 agglomerates when the stabilizing agent sodium pyrophosphate was used. TEM results revealed that the resulting nanoparticles were well-dispersed, spherical, and less than 200 nm in diameter. The diameter (d_p) of Ccm-NPs ranged between 26 and 93 nm, with an average size ($\overline{d_p}$) of ∼53 nm (Figure 5 and Table 1). For ADP-NPs, slightly larger particles were obtained, with a size range of ∼32−160 nm and an average diameter of ∼77 nm (Figure 5 and Table 1). Note that all particle sizes were statistically determined from multiple TEM images at the same magnification (12000×). DLS analysis of stabilized nanoparticles showed (i) bidispersity; binomial size distribution of Ccm-NPs, with a hydrodynamic diameter (d_h) range of 44−712 nm and a mean hydrodynamic size ($\overline{d_h}$) of 43 and 425 nm; and (ii) polydispersity; trinomial size distribution of ADP-NPs, with a d_h range of 91−5560 nm and $\overline{d_h}$ of 125, 492, and 4835 nm (Figure 6 and Table 1). DLS results yielded a broader size range of nanoparticles because, unlike TEM, this technique cannot be used to distinguish between individual particles and agglomerates. Accordingly, the larger measured sizes obtained from DLS were primarily caused by the agglomeration of Ccm-NPs and ADP-NPs. The actual concentrations

Table 3. Antioxidant Activities of BHA, BHT, Ccm-EtOH, Ccm-H_2O, Ccm-NPs, ADP-EtOH, ADP-H_2O, and ADP-NPs[a]

	radical scavenging; EC_{50} ($\mu g\ mL^{-1}$)		antioxidant activities	
antioxidants	DPPH scavenging	ABTS scavenging	β-carotene bleaching (%)	FRAP (TE $\mu M\ mL^{-1}$)
BHA	1.22 ± 0.77 f	3.86 ± 0.96 h	92.12 ± 2.72 a	869.38 ± 1.34 a
BHT	2.47 ± 1.09 ef	140.82 ± 1.72 f	34.16 ± 2.49 d	16.97 ± 3.40 d
Ccm-EtOH	3.96 ± 1.11 e	228.68 ± 1.26 e	39.89 ± 2.04 c	23.03 ± 2.61 c
Ccm-H_2O	51.09 ± 1.40 c	349.32 ± 1.50 c	9.58 ± 1.90 e	ND
Ccm-NPs	2.93 ± 0.61 ef	51.34 ± 1.30 g	49.23 ± 6.44 b	56.88 ± 2.56 b
ADP-EtOH	29.12 ± 0.99 d	343.46 ± 0.92 d	3.06 ± 0.26 f	ND
ADP-H_2O	123.39 ± 1.27 a	509.84 ± 1.33 a	ND	ND
ADP-NPs	76.32 ± 0.71 b	355.40 ± 1.26 b	1.22 ± 0.87 f	ND

[a](a−f) Means within the same column and the same main effect with different superscript letters are different ($p \leq 0.05$). ND: values are not quantifiable due to lack of dose-response.

of Ccm-NPs and ADP-NPs in 0.1 wt % F127 solutions, determined by UV−vis spectrophotometry, were 0.811 ± 0.04 and 0.663 ± 0.02 mg mL^{-1}, respectively. In methyl cellulose solutions, the actual concentrations of Ccm and ADP nanoparticles were 1.14 ± 0.01 and 2.10 ± 0.08 mg mL^{-1}, respectively (Table 2).

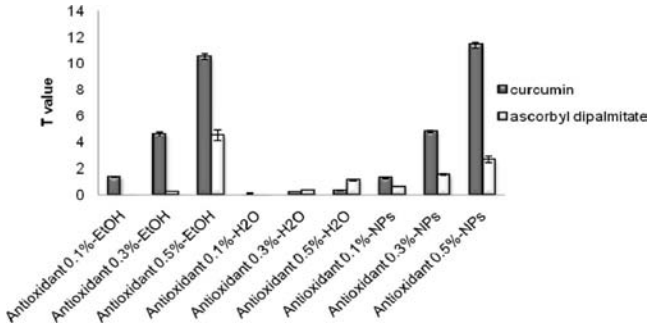

Figure 7. Light absorbance (T value) at 427 and 254 nm, respectively, of curcumin and ascorbyl dipalmitate incorporated into films at 0.1, 0.3, and 0.5 wt %.

Radical Scavenging and Antioxidant Activities. *DPPH Radical Scavenging.* The total radical scavenging capacity of the tested compounds (Ccm-EtOH, Ccm-H_2O, Ccm-NPs, ADP-EtOH, ADP-H_2O, and ADP-NPs) were determined and compared to those of BHA and BHT by using DPPH radical scavenging methods. There was a highly statistically significant difference between the mean DPPH radical scavenging values ($p < 0.01$). Table 3 shows that BHA and BHT had higher radical scavenging activity, with lower EC_{50} of 1.22 and 2.47 μg mL^{-1}, respectively. The lower EC_{50} value indicated a higher DPPH free radical scavenging effectiveness. In the case of Ccm solutions, EC_{50} for Ccm-H_2O was 51.09 μg mL^{-1}, which indicated a lower radical scavenging activity than those of Ccm-EtOH and Ccm-NPs, with EC_{50} of 3.96 and 2.93 μg mL^{-1}, respectively. The results indicated that Ccm-NPs had higher radical scavenging values than Ccm-H_2O. In the case of ADP

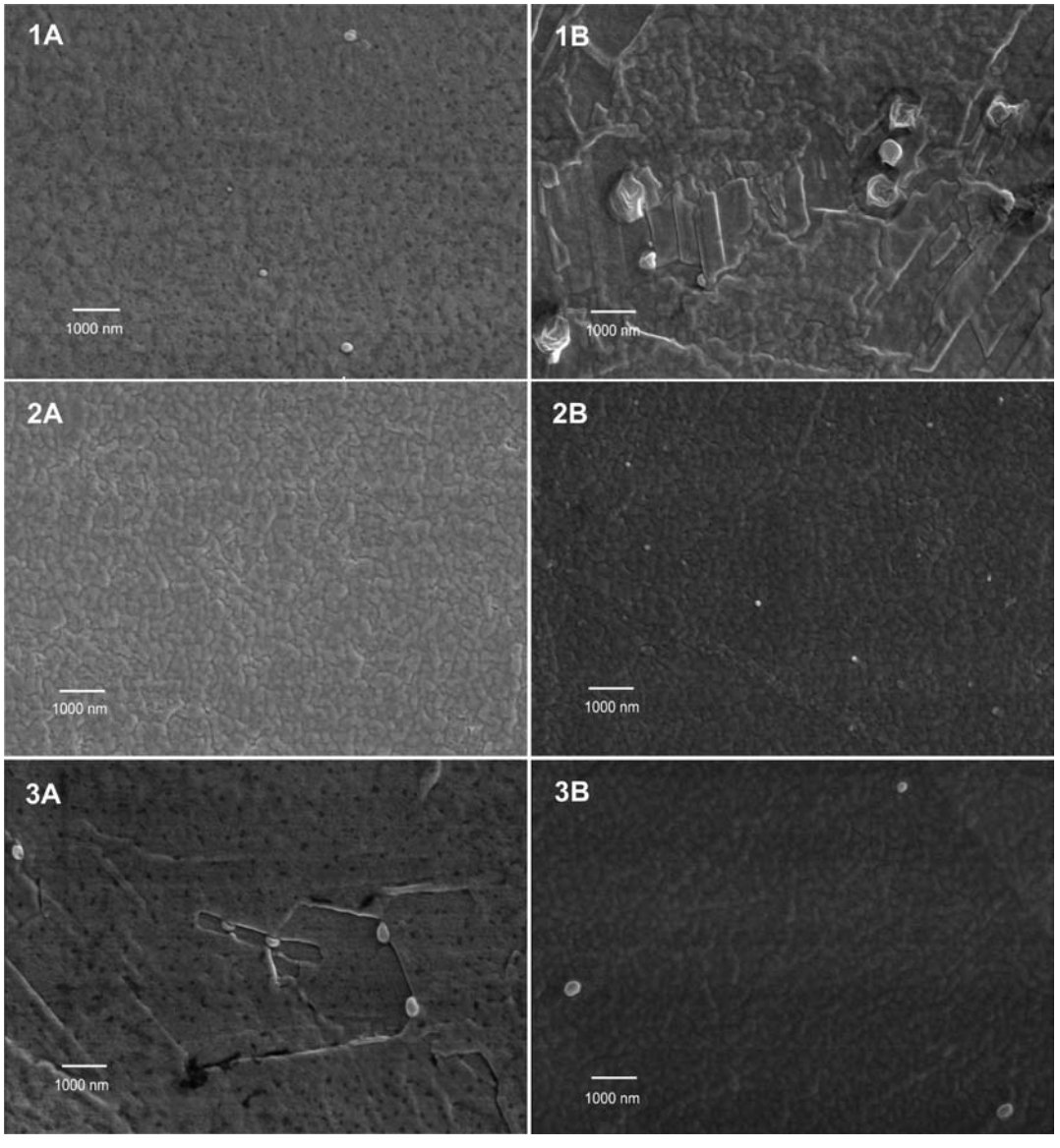

Figure 8. Scanning electron micrographs of 0.5 wt % substance-incorporated methyl cellulose films at 10000×: (1A) Ccm in EtOH; (2A) Ccm in H_2O; (3A) Ccm-NPs in methyl cellulose; (1B) ADP in EtOH; (2B) ADP in H_2O; (3B) ADP-NPs in methyl cellulose.

dx.doi.org/10.1021/jf301311g | J. Agric. Food Chem. 2012, 60, 5388−5399

Table 4. Antioxidant Activities of Cellulose-Based Films Containing BHA, BHT, Ccm-EtOH, Ccm-H_2O, Ccm-NPs, ADP-EtOH, ADP-H_2O, and ADP-NPs[a]

antioxidants	concentration (% w/w)	DPPH scavenging (%)	ABTS scavenging (%)	β-carotene bleaching (%)	FRAP (TE μM mL^{-1})
BHA	0.1	10.06 ± 0.71 j	22.09 ± 1.89 f	14.98 ± 0.33 f	2.70 ± 0.31 h
	0.3	41.17 ± 0.71 e	31.31 ± 0.83 e	42.96 ± 1.27 b	17.09 ± 2.74 g
	0.5	43.55 ± 0.39 d	48.28 ± 3.20 d	50.00 ± 0.89 a	21.00 ± 2.80 f
BHT	0.1	1.95 ± 0.67 L	7.03 ± 0.60 jk	1.10 ± 0.80 L	ND
	0.3	2.62 ± 0.57 L	8.76 ± 0.83 ijk	2.33 ± 0.56 L	ND
	0.5	5.97 ± 1.72 k	10.75 ± 1.74 i	6.98 ± 0.47 hi	ND
Ccm-EtOH	0.1	14.65 ± 1.08 h	22.85 ± 1.69 f	8.53 ± 0.05 h	15.87 ± 0.09 g
	0.3	34.04 ± 0.40 f	60.92 ± 1.31 c	11.59 ± 4.49 g	57.14 ± 0.14 d
	0.5	56.45 ± 0.62 b	73.15 ± 0.58 b	25.32 ± 2.17 d	77.66 ± 2.97 b
Ccm-H_2O	0.1	2.96 ± 0.87 L	8.57 ± 0.04 ijk	3.05 ± 0.22 kl	ND
	0.3	12.64 ± 0.25 i	13.23 ± 0.04 h	4.60 ± 0.37 jk	ND
	0.5	16.40 ± 1.68 h	15.56 ± 0.46 g	6.18 ± 1.28 ij	ND
Ccm-NPs	0.1	30.01 ± 4.60 g	33.30 ± 1.79 e	7.80 ± 1.81 hi	25.71 ± 0.11 f
	0.3	48.63 ± 1.10 c	74.92 ± 1.17 b	21.89 ± 0.56 e	74.14 ± 0.05 c
	0.5	59.95 ± 0.18 a	97.23 ± 0.87 a	33.73 ± 0.09 c	152.47 ± 0.14 a
ADP-EtOH	0.1	ND	3.39 ± 0.02 L	ND	ND
	0.3	ND	6.75 ± 1.23 k	ND	ND
	0.5	ND	9.32 ± 1.68 ij	ND	ND
ADP-H_2O	0.1	ND	ND	ND	ND
	0.3	ND	ND	ND	ND
	0.5	ND	ND	ND	ND
ADP-NPs	0.1	2.37 ± 1.15 L	8.79 ± 0.90 ijk	ND	ND
	0.3	6.71 ± 0.90 k	10.20 ± 0.04 i	ND	ND
	0.5	7.59 ± 0.11 k	10.40 ± 0.22 i	ND	ND

[a](a–l) Means within the same column and the same main effect with different superscript letters are different ($p \leq 0.05$). ND: values are not quantifiable due to lack of dose-response.

solutions, EC_{50} for ADP-H_2O was 123.39 μg mL^{-1}, which indicated lower radical scavenging activity than ADP-EtOH and ADP-NPs, with EC_{50} of 29.12 and 76.32 μg mL^{-1}, respectively. Ccm-NPs were better than Ccm-EtOH and Ccm-H_2O, whereas ADP-NPs were better than ADP-H_2O, at scavenging DPPH free radicals. This is due to the increased particle distribution and smaller size of Ccm-NPs and ADP-NPs, so that the surface area and area reaction are increased.[13] In addition, Pluronic F127 inhibits particle aggregation and agglomeration and improves distribution of particles.[14] This finding is in agreement with the study by Bao et al.,[24] which reported that the addition of tea polyphenol-loaded chitosan nanoparticles could improve the antioxidant activity of gelatin film, and the study by Huang et al.,[11] which reported that selenium nanoparticles (Nano-Se) had one potential size-dependent sequence in both free radical scavenging and antioxidant effects. The smaller the particle, the better the effects at low concentration. As a stable nitrogen-centered free radical, the DPPH model system is a widely used assay to evaluate antioxidant activity and is comparatively rapid as opposed to other methods.[35] The addition of antioxidants to the DPPH solution resulted in a rapid decrease in the optical density at 517 nm. The extent of discoloration indicates the scavenging capacity of the antioxidant.[36] The antioxidant reduces the DPPH radical from a dark purple-colored compound to a light yellow-colored compound, diphenyl-picryl hydrazine; the degree of the reaction relies on the hydrogen- or electron-donating ability of the antioxidant.[37,38] The method is based on the reduction of DPPH in the presence of a hydrogen-donating antioxidant, due to the formation of the nonradical form DPPH-H in the reaction. DPPH in unstable form was donated an electron or hydrogen atom by Ccm, either from the enol form between the molecule's methoxyphenol

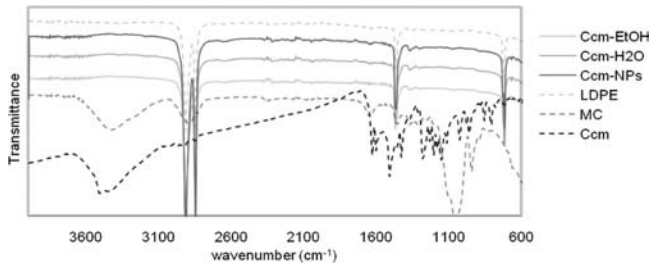

Figure 9. Infrared spectra of curcumin powder (Ccm), methyl cellulose (MC), LDPE, and 0.5 wt % of Ccm-EtOH, Ccm-H_2O, and Ccm-NPs methyl cellulose-based films.

rings, or from hydroxyl groups in the phenolic rings.[7,39,40] Then, Ccm was tautomerized into both keto forms between methoxyphenol rings and stabilized as radical resonance in phenolic rings. Although the mechanism of ADP action in this method is not known, perhaps the most likely explanation is that ADP reacts with free-radical species as they are formed. ADP can react with free-radical species in the same manner as an ascorbic acid reaction.[41,42] Substances which enable the performance of this reaction can be considered as antioxidants and therefore radical scavengers.[43] EC_{50} of ADP-NPs had less radical scavenging capacity than ADP-EtOH because ADP-NPs in nanosuspension can unfortunately agglomerate into a larger particle size. Nevertheless, ADP-NPs with a smaller particle size could improve radical scavenging from an aqueous solution.

ABTS Radical Cation Scavenging. ABTS radical cation scavenging activity is shown in Table 3. Similar to DPPH radical scavenging values, there was a highly statistically significant difference between the mean ABTS radical cation scavenging values ($p < 0.01$). The results showed that BHA had a high

dx.doi.org/10.1021/jf301311g | J. Agric. Food Chem. 2012, 60, 5388–5399

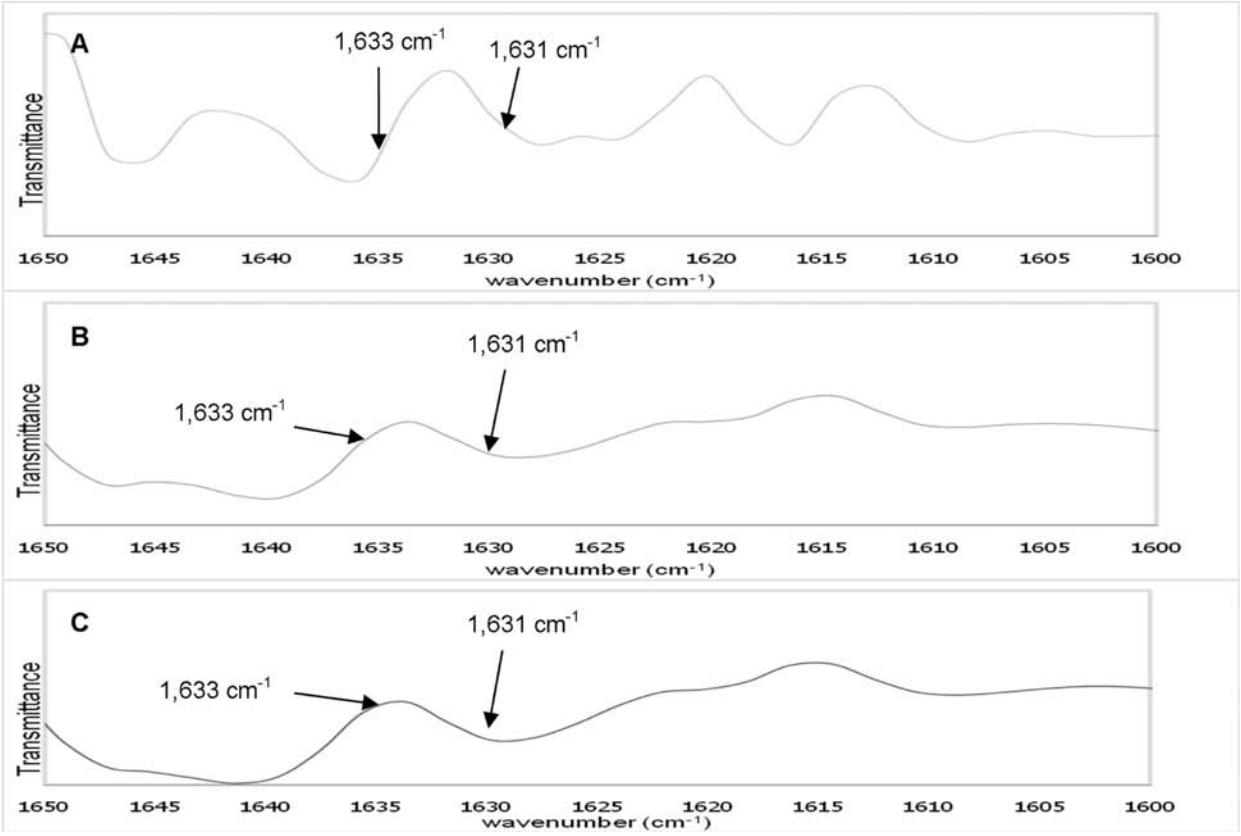

Figure 10. Infrared spectra of Ccm-EtOH (A), Ccm-H_2O (B), and Ccm-NPs (C) methyl cellulose-LDPE-based films. A strong band at 1631 cm^{-1} can be assigned to ν(C═C) of the benzene ring, and a high frequency band of C═O vibrations of the diketo form at 1633 cm^{-1}.

radical scavenging activity, with EC_{50} of 3.86 μg mL^{-1}, which was superior to those of other substances. In the case of Ccm solutions, EC_{50} for Ccm-H_2O was 349.32 μg mL^{-1}, which indicated a lower radical scavenging activity than Ccm-EtOH and Ccm-NPs, with EC_{50} of 228.68 and 51.34 μg mL^{-1}, respectively. Ccm-NPs had better radical scavenging activity than Ccm-H_2O and BHT solutions, with EC_{50} of 349.32 and 140.82 μg mL^{-1}, respectively. In the case of ADP solutions, EC_{50} for ADP-H_2O was 509.84 μg mL^{-1}, which indicated a lower radical scavenging activity than ADP-EtOH and ADP-NPs, with EC_{50} of 343.46 and 355.40 μg mL^{-1}, respectively. ADP-NPs showed a similar trend to DPPH radical scavenging activity.

The ABTS radical cation is more reactive than the DPPH radical, which involves H-atom transfer and electron-transfer processes. The blue-green ABTS radical cation solution was prepared via a reaction between ABTS and potassium persulfate; the ABTS radical cation was generated by potassium persulfate oxidation. Bleaching of a blue-green ABTS solution has been used to evaluate the antioxidant capacity of individual compounds. The ABTS radical cation is bleached by the H-atom and the electron transfer mechanism from the functional groups of Ccm and ADP, similar to the case of a DPPH reaction.[7,39,41,42]

β-Carotene Linoleate Oxidative Bleaching. As shown in Table 3, there was a highly statistically significant difference between the mean β-carotene linoleate oxidative bleaching values ($p < 0.01$). In the case of BHA solution, the mean β-carotene linoleate oxidative bleaching value (92.12%) was higher than those of other substances. With Ccm solutions, Ccm-NPs had a higher β-carotene linoleate oxidative bleaching value (49.23%) than Ccm-H_2O (9.58%), Ccm-EtOH (39.89%), and BHT (34.16%) solutions. In the case of ADP solutions, ADP-EtOH had a higher β-carotene linoleate oxidative bleaching value (3.06%) than ADP-H_2O (no data) and ADP-NPs (1.22%); this indicated that ADP-NPs with a smaller particle size in an aqueous solution could improve β-carotene linoleate oxidative bleaching (Table 3).

The β-carotene linoleate oxidative bleaching assay is a commonly used model to evaluate the antioxidant capacity of plant extracts because β-carotene is extremely sensitive to free radical mediated oxidation of linoleic acid. Linoleic acid, an unsaturated fatty acid, can produce the reactive oxygen species formed from halogenated water. The reactive oxygen species will initiate β-carotene oxidation, leading to discoloration of β-carotene. Thus, the results of inhibition of β-carotene bleaching show that Ccm and ADP are able to quench and scavenge singlet oxygen in this mechanism.[42,44−46]

Ferric Reducing Antioxidant Power. As shown in Table 3, there was a highly statistically significant difference between the mean ferric reducing antioxidant power values ($p < 0.01$). BHA solution showed the highest ferric reducing antioxidant power (FRAP) of 869.38 μM mL^{-1}, followed by Ccm-NPs (56.88 μM mL^{-1}), Ccm-EtOH (23.03 μM mL^{-1}), and BHT (16.97 μM mL^{-1}). But all solution values for Ccm-H_2O and ADP were not quantifiable due to the lack of dose−response. It has been suggested that the antioxidant activity of Ccm depends upon the presence of phenolic functional groups.[39,47] However, other studies support the conclusion that the central methylene hydrogens of curcumin are important for antioxidant activity.[40] It has since been demonstrated that both central methylene hydrogens and phenolic hydrogens may be involved in the

dx.doi.org/10.1021/jf301311g | J. Agric. Food Chem. 2012, 60, 5388−5399

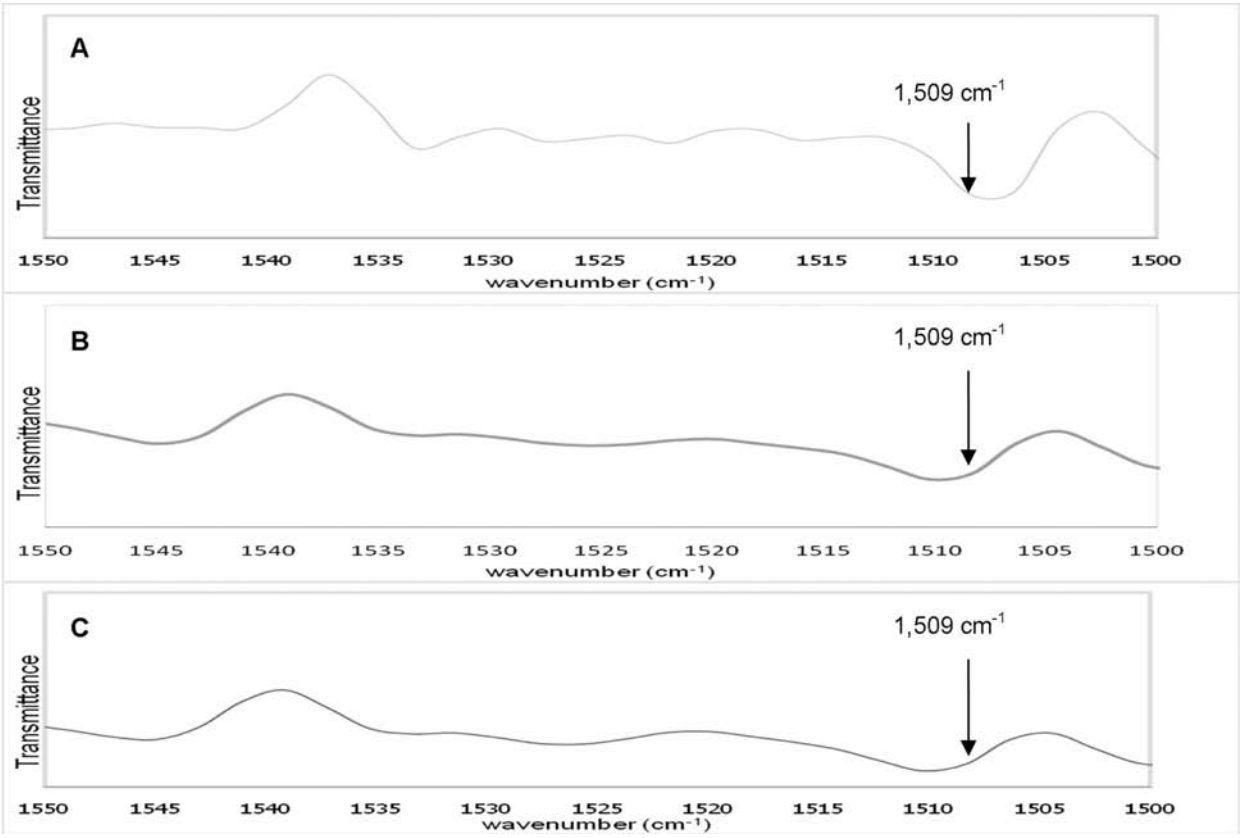

Figure 11. Infrared spectra of Ccm-EtOH (A), Ccm-H_2O (B), and Ccm-NPs (C) methyl cellulose-LDPE-based films, showing a high frequency mixed vibration of C═C and C−O at 1509 cm^{-1}.

mechanism of formation of the phenoxy radical, depending upon reaction conditions.[48,49]

During the reducing power assay, the presence of reductants (antioxidants) in the tested samples reduced the Fe^{3+}-TPTZ complex to the ferrous form (Fe^{2+}). Gordon[50] reported that the antioxidant action of reductions is based on breaking of the radical chain by donation of a hydrogen atom. In addition, the FRAP assay can provide information on total antioxidant potential in cells in a relatively short time without having to run more lengthy tests for each individual antioxidant.[51] However, there are some pitfalls to this assay that need to be discussed. Apart from determining the potential of biological antioxidants, it also determines chemical reductants that reduce the ferric complex to the ferrous form, and not all of these reductants are antioxidant. This assay does not account for the −SH groups of antioxidants.[52] For instance, the antioxidant glutathione (GSH) is not able to reduce Fe^{3+}.

Ccm-NPs- and ADP-NPs−Incorporated Methyl Cellulose Film Samples. There was no statistical difference in the thickness of the different films. They varied from 50 to 60 μm. Figure 7 shows the UV−visible light absorbance of films, with Ccm λ_{max} at 427 nm and ADP at 254 nm. Scanning electron micrographs of various types of Ccm and ADP solutions (0.5 wt %) in methyl cellulose films at magnifications of 10000× are illustrated in Figure 8. It was found that cellulose-based film containing 0.5 wt % Ccm-EtOH had particle sizes of less than 1000 nm on the surface of the film, similar to 0.5 wt % Ccm-NPs-incorporated cellulose-based film. Cellulose-based film containing 0.5 wt % Ccm-H_2O did not yield Ccm particles on its surface because only the supernatant of the Ccm solution was incorporated into the methyl cellulose solution, and thus the particles do not appear. Cellulose-based film containing 0.5 wt % ADP-EtOH had particles larger than 1000 nm in size on its surface. In the case of ADP-H_2O, it was found that film incorporated with the supernatant of the ADP solution had particle sizes of less than 1000 nm — smaller than ADP-NPs particle sizes. However, the ADP-NPs films showed higher radical scavenging activity for all treatments than those of ADP-EtOH and ADP-H_2O films (Table 4).

Radical Scavenging and Antioxidant Activities of Films. The findings showed that DPPH radical scavenging and ABTS radical cation scavenging activities of the films significantly increased ($p < 0.01$) with increasing antioxidant concentration, as shown in Table 4. The DPPH radical scavenging activity of methyl cellulose films incorporated with Ccm-NPs was monitored in comparison with synthetic reference antioxidants. As the Ccm-NPs increased in the film formulation, this antioxidant activity tended to increase, as did the expected antioxidant property of the bioactive film. In terms of the DPPH radical scavenging activity and ABTS radical cation scavenging activity of the ADP films, ADP-NPs showed higher activity than ADP-H_2O film, but ADP-NPs film revealed less activity than ADP-EtOH film due to the ADP particle size in ADP-EtOH film, which allowed particles to be rapidly released into test solutions.

The results revealed that antioxidant activity of the films against β-carotene linoleate oxidative bleaching and FRAP assays significantly increased ($p < 0.01$) with increasing antioxidant concentration (Table 4). With concentrations of 0.1−0.5 wt %, Ccm-NPs-incorporated methylcellulose films revealed β-carotene linoleate bleaching and FRAP values in ranges of 7.80−33.78% and 25.71−152.47 μM mL^{-1}, respectively. In all cases of ADP

films, no activity was found by the β-carotene linoleate bleaching assay. FRAP values were not quantifiable due to lack of dose−response. Additionally, ADP could be degraded by light and temperature. So in applications with ADP, controlled release activities could be improved by encapsulation.[15]

FTIR Spectra. FTIR spectroscopy was employed as a tool for investigating the functional groups among methyl cellulose film, LDPE film, Ccm and ADP powders, Ccm-EtOH, Ccm-H_2O, Ccm-NPs, ADP-EtOH, ADP-H_2O, and ADP-NPs films by measuring absorbance over a wavenumber range of 4000−600 cm^{-1} at a resolution of 4 cm^{-1}. The chemical structures of Ccm and ADP are presented in Figure 1. The impregnation of Ccm and ADP into methyl cellulose films on LDPE substrate films is confirmed by FTIR spectra (Figures 9−12).

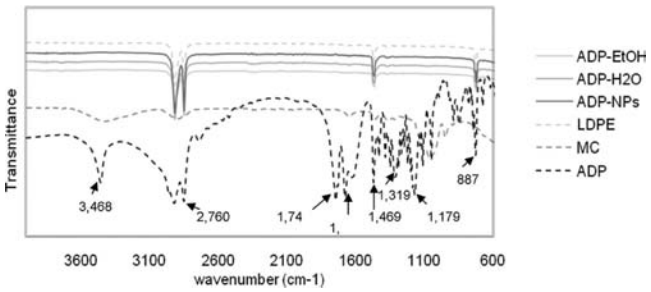

Figure 12. Infrared spectra of ascorbyl dipalmitate (ADP) powder, methyl cellulose (MC), LDPE, and 0.5 wt % of ADP-EtOH, ADP-H_2O, and ADP-NPs methyl cellulose-LDPE-based films, showing a high frequency region of C−O at about 1000−1300 cm^{-1} for determining the functional group of ester.

In Figure 9, LDPE film has methylene stretches at 2920 cm^{-1} and 2850 cm^{-1}; moreover, it has methylene deformations (bending of CH_2) at 1464 cm^{-1} and rocking of CH at 719 cm^{-1}.[53] Methyl cellulose showed high frequency C−O stretching at about 1076 cm^{-1}.[54] The highest frequency region of phenolic ν(OH) vibrations of Ccm was calculated by Kolev et al.[55] at 3595 cm^{-1}, but in practice this band could be shifted downward due to the intramolecular and intermolecular hydrogen bonds.[56] This ν(OH) sharp band at 3522 cm^{-1} was observed. Moreover, for enolic ν(OH) mode, the theoretical spectrum predicts a strong band at 2962 cm^{-1}. In Figure 10, the diketo form of Ccm is preferred in solid phase and the enol form in solution. In the middle region, a strong band at 1631 cm^{-1} can be assigned to ν(C═C) of the benzene ring. The observed shoulder at 1633 in the infrared (IR) spectrum is a characteristic band of C═O vibrations of the diketo form. The most prominent band in the IR spectrum was at 1509 cm^{-1}. All films containing either Ccm-EtOH, Ccm-H_2O, or Ccm-NPs revealed prominent bands at 1509 cm^{-1}, corresponding to intermolecular and intermolecular conjugation (Figure 11), which are attributed to highly mixed vibrations between ν(C═C) and ν(C═O) of the benzene ring. A very clear band at 1429 cm^{-1} was assigned to deformation vibrations of the two methyl groups. One prominent band at 1155 cm^{-1} was assigned to (C−O−C) vibration. The IR bands at 1028 and 812 cm^{-1} could be assigned to ν(C−H) out-of-plane vibration of the aromatic ring.[56] The highest frequency region of O−H stretching of ADP was at 3468 cm^{-1}. Functional C═O groups of pure ADP were located at 1745 cm^{-1} and 1678 cm^{-1} (Figure 12). A very clear band at 1469 cm^{-1} was assigned to deformation

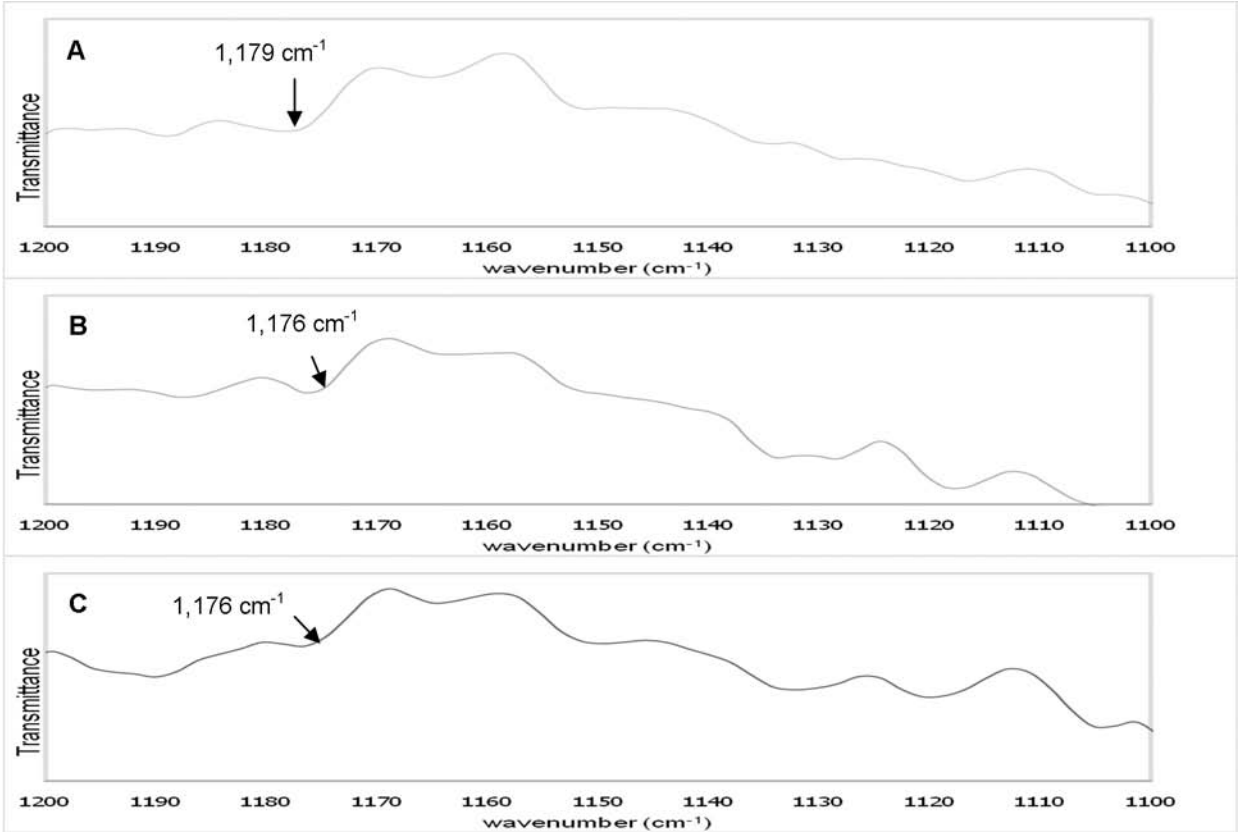

Figure 13. Infrared spectra of ADP-EtOH (A), ADP-H_2O (B), and ADP-NPs (C) methyl cellulose-LDPE-based films, showing a high frequency region of C−O at about 1000−1300 cm^{-1} for determining the functional group of ester at 1179 cm^{-1}.

dx.doi.org/10.1021/jf301311g | J. Agric. Food Chem. 2012, 60, 5388−5399

vibrations of the two methyl groups. The ADP films had a high frequency region with C−O about 1000−1300 cm^{-1} for determining the functional group of ester at 1176−1179 cm^{-1} (Figure 13).[57]

In this work, Ccm-NPs and ADP-NPs were successfully produced in a single step using the RESOLV technique. Ccm-NPs and ADP-NPs stabilized in either Pluronic F127 or methyl cellulose solution were well-dispersed, spherical, and individual NPs with average sizes of ∼50 and ∼80 nm, respectively. Ccm-NPs and ADP-NPs showed higher antioxidant activities to inhibit the oxidation of β-carotene, scavenge DPPH and ABTS free radicals, and reduce the ferric complex to the ferrous form than those of Ccm and ADP. This work also demonstrates that the AO components of Ccm and ADP can be nanoparticulated and incorporated into cellulose-based biopolymers while retaining their antioxidant activities. Cellulose-based edible films could act as reservoirs and release Ccm and ADP to maintain an inhibitory effect at the food surface. This demonstrates a promising potential use of Ccm-NPs and ADP-NPs for application in antioxidant packaging films and coatings.

AUTHOR INFORMATION

Corresponding Author

*E-mail: fagipas@ku.ac.th.

Funding

This work was supported by the Commission on Higher Education, Ministry of Education, Thailand (National Research University of Thailand) and the Office of National Research Council of Thailand.

Notes

The authors declare no competing financial interest.

ACKNOWLEDGMENTS

The authors gratefully acknowledge Assoc. Prof. Voraphat Luckanatinvong with Department of Agricultural Technology, Thammasat University, and Prof. Jumras Limtrakul, Department of Chemistry, Kasetsart University, for their support toward the experiments. The authors acknowledge the National Nanotechnology Center (NANOTEC), the National Science and Technology Development Agency (NSTDA), and the Ministry of Science and Technology of Thailand through its NANOTEC Center of Excellence for supporting research equipment. The authors are also thankful to Ms. Thikhamporn Noiklam, Department of Packaging and Materials Technology, Kasetsart University, for preparing Ccm and ADP nanoparticles.

REFERENCES

(1) Decker, E. A.; Chan, W. K. M.; Livisay, S. A.; Butterfield, D. A.; Faustman, C. Interactions between carnosine and the different redox states of myoglobin. *J. Food Sci.* **1995**, *60*, 1201−1204.

(2) Davies, K. J. A. Oxidative stress: the paradox of aerobic life. In *Free Radicals and Oxidative Stress: Environment, Drugs and Food Additives*; Rice-Evans, C., Halliwell, B., Lunt, G. G., Eds.; Biochemical Society Symposium; Portland Press: London, 1995; Vol. *61*, pp 1−31.

(3) Botterweck, A. A. M.; Verhagen, H.; Goldbohm, R. A.; Kleinjans, J.; Van den Bradt, P. A. Intake of butylated hydroxyanisole and butylated hydroxytoluene and stomach cancer risk: results from analyses in the Netherlands cohort study. *Food Chem. Toxicol.* **2000**, *38*, 599−605.

(4) Ito, N.; Hirose, M.; Fukushima, H.; Tsuda, T.; Shirai, T.; Tatenatsu, M. Studies on antioxidants: Their carcinogenic and modifying effects on chemical carcinogens. *Food Chem. Toxicol.* **1986**, *24*, 1071−1092.

(5) Plumb, G. W.; Chambers, S. J.; Lambert, N.; Bartolomé, B.; Heaney, R. K.; Wanigatunga, S.; Aruoma, O. I.; Halliwell, B.; Williamson, G. Antioxidant actions of fruit, herb and spice extracts. *J. Food Lipids.* **1996**, *3*, 171−188.

(6) Cousins, M.; Adelberg, J.; Chen, F. Antioxidant capacity of fresh and dried rhizomes from four clones of turmeric (*Curcuma longa* L.) grown in vitro. *Ind. Crop. Prod.* **2007**, *25*, 129−135.

(7) Ak, T.; Gülçin, I. Antioxidant and radical scavenging properties of curcumin. *Chem. Biol. Int.* **2008**, *174*, 27−37.

(8) Moribe, K.; Maruyama, S.; Inoue, Y.; Suzuki, T.; Fukami, T.; Tomono, K.; Higashi, K.; Tozuka, Y.; Yamamoto. Ascorbyl dipalmitate/PEG-lipid nanoparticles as a novel carrier for hydrophobic drugs. *Int. J. Pharm.* **2010**, 236−243.

(9) Robinson, D. K. R.; Morrison, M. J. Nanotechnologies for food packaging: Reporting the science and technology research trends: Report for the Observatory NANO, 2010. http://www.observatorynano.eu (accessed July 11, 2011).

(10) Chaudhry, Q.; Castle, L. Food applications of nanotechnologies: An overview of opportunities and challenges for developing countries. *Trends Food Sci. Technol.* **2011**, *22*, 595−603.

(11) Huang, B.; Zhang, J.; Hou, J.; Chen, C. Free radical scavenging efficiency of Nano-Se in vitro. *Free Radical Biol. Med.* **2003**, *35*, 805−813.

(12) Liu, J.−R.; Chen, J.−F.; Shin, H. N.; Kuo, P. C. Enhanced antioxidant bioactivity of *Salvia miltiorrhiza* (Danshen) products prepared using nanotechnology. *Phytomedicine* **2008**, *15*, 23−30.

(13) Mohoraj, V. J.; Chen, Y. Nanoparticles − a review. *Trop. J. Pharm. Res.* **2006**, *5*, 561−573.

(14) Sane, A.; Thies, M. C. The formation of fluorinated tetraphenylporphyrin nanoparticles via rapid expansion processes: RESS vs RESOL. *J. Phys. Chem. B.* **2005**, *109*, 19688−19695.

(15) Sane, A.; Limtrakul, J. Formation of retinyl palmitate-loaded poly(l-lactide) nanoparticles using rapid expansion of supercritical solutions into liquid solvents (RESOLV). *J. Supercrit. Fluids* **2009**, *17*, 111−134.

(16) Sane, A.; Limtrakul, J. Co-precipitation of asiatic acid and poly(l-lactide) using rapid expansion of subcritical solutions into liquid solvents. *J. Nanoparticle Res.* **2011**, *13*, 4001−4013.

(17) Kester, J. J.; Fennema, O. R. Edible films and coatings: a review. *Food Technol.* **1986**, *40*, 47−59.

(18) Suppakul, P.; Miltz, J.; Sonneveld, K.; Bigger, S. W. Active packaging technologies with an emphasis on antimicrobial packaging and its applications. *J. Food Sci.* **2003**, *68*, 408−420.

(19) Nicholson, M. D. The role of natural antimicrobials in food/packaging biopreservation. *J. Plastic Film Sheeting* **1998**, *14*, 234−241.

(20) Wessling, C.; Nielsen, T.; Giacin, J. R. Antioxidant ability of BHT- and α-tocopherol-impregnated LDPE film in packaging of oatmeal. *J. Sci. Food Agric.* **2000**, *81*, 194−201.

(21) Lee, Y. S.; Shin, H.-S.; Han, J.-K.; Lee, M.; Giacin, J. R. Effectiveness of antioxidant-impregnated film in retarding lipid oxidation. *J. Sci. Food Agric.* **2000**, *84*, 993−1000.

(22) Jongjareonrak, A.; Benjakul, S.; Visessanguan, W.; Tanaka, M. Antioxidative activity and properties of fish skin gelatin films incorporated with BHT and α-tocopherol. *Food Hydrocolloids* **2008**, *22*, 449−458.

(23) Siripatrawan, U.; Harte, B. R. Physical properties and antioxidant activity of an active film from chitosan incorporated with green tea extract. *Food Hydrocolloids* **2010**, *24*, 770−775.

(24) Bao, S.; Xu, S.; Wang, Z. Antioxidant activity and properties of gelatin films incorporated with tea polyphenol-loaded chitosan nanoparticles. *J. Sci. Food Agric.* **2009**, *89*, 2692−2700.

(25) Rejinold, N. S.; Muthunarayanan, M.; Divyarani, V. V.; Sreerekha, P. R.; Chemnazhi, K. P.; Nair, S. V.; Tamura, H.; Jayakumar, R. Curcumin-loaded biocompatible thermoresponsive polymer nanoparticles for cancer drug delivery. *J. Colloid Interface Sci.* **2011**, *1*, 39−51.

(26) Berne, B. J.; Pecora, R. *Dynamic Light Scattering: with Applications to Chemistry, Biology, and Physics*; Dover Publications: Mineola, NY, 2000.
(27) Bootz, A.; Vogel, V.; Schubert, D.; Kreuter, J. Comparison of scanning electron microscopy, dynamic light scattering and analytical ultracentrifugation for the sizing of poly(butyl cyanoacrylate) nanoparticles. *Eur. J. Pharm. Biopharm.* **2004**, *57*, 369−375.
(28) Yen, F.-L.; Wu, T.-H.; Tzeng, C.-W.; Lin, L.-T.; Lin, C.-C. Curcumin nanoparticles improve the physicochemical properties of curcumin and effectively enhance its antioxidant and antihepatoma activities. *J. Agric. Food Chem.* **2010**, *58*, 7376−7382.
(29) Xiao, H.; Parkin, K. L. Antioxidant functions of selected allium thiosulfinates and S-alk(en)yl-L-cysteine sulfoxides. *J. Agric. Food Chem.* **2002**, *50*, 2488−2493.
(30) Singh, R. P.; Chidambara, M. K. N.; Jayaprakasha, G. K. Studies on the antioxidant activity of pomegranate (*Punica granatum*) peel and seed extracts using in vitro models. *J. Agric. Food Chem.* **2002**, *50*, 81−86.
(31) Terpinc, P.; Bezjak, M.; Abramovic, H. A kinetic model of evaluation of the antioxidant activity of several rosemary extracts. *Food Chem.* **2009**, *115*, 740−744.
(32) Benzie, I. F. F.; Strain, J. J. The ferric reducing ability of plasma (FRAP) as a measure of "antioxidant power": the FRAP assay. *Anal. Biochem.* **1996**, *239*, 70−76.
(33) Thaipong, K.; Boonprakob, U.; Crosby, K.; Cisneros-Zevallos, L.; Byrne, D. H. Comparison of ABTS, DPPH, FRAP, and ORAC assays for estimating antioxidant activity from guava fruit extracts. *J. Food Compos. Anal.* **2006**, *19*, 669−675.
(34) Jiang, J; Oberdörster, G.; Biwas, P. Characterization of size, surface charge, and agglomeration state of nanoparticle dispersion for toxicological studies. *J. Nanoparticle Res.* **2009**, *11*, 77−89.
(35) Gülçin, İ.; Şat, İ.G.; Beydemir, Ş.; Elmastaş.; Küfrevioğlu, Ö.İ. Comparison of antioxidant activity of clove (*Eugenia caryophyllata* Thunb.) buds and lavender (*Lavandula stoechas* L.). *Food Chem.* **2004**, *87*, 393−400.
(36) Enayat, S.; Banerjee, S. Comparative antioxidant activity of extracts from leaves, bark and catkins of *Salix aegyptiaca* sp. *Food Chem.* **2009**, *116*, 23−28.
(37) Blois, M. S. Antioxidant determinations by the use of a stable free radical. *Nature* **1958**, *181*, 1199−1200.
(38) Brand−Williams, W.; Cuvelier, M.; Berset, C. Use of a free radical method to evaluate antioxidant activity. *Lebensm.-Wiss. u.-Technol.* **1995**, *28*, 25−30.
(39) Priyadarsini, K. I.; Maity, D. K.; Naik, G. H.; Kumar, M. S.; Unnikrishnan, M. K.; Satav, J. G.; Mohan, H. Role of phenolic O−H and methylene hydrogen on the free radical reactions and antioxidant activity of curcumin. *Free Radical Biol. Med.* **2003**, *35*, 475−484.
(40) Jovanovic, S. V.; Boone, C. W.; Steenken, S.; Trinoga, M.; Kaskey, R. B. How curcumin works preferentially with water soluble antioxidants. *J. Am. Chem. Soc.* **2001**, *123*, 3064−3068.
(41) Coppen, P. The use of antioxidants. In *Rancidity in Foods*, 3rd ed.; Allen, J. C. Hamilton, R. J., Eds.; Blackie Academic Press: London, 1994; pp 84−103.
(42) Beddows, C. G.; Jagait, C.; Kelly, M. J. Effect of ascorbyl palmitate on preservation of α-tocopherol in sunflower oil, alone and with herbs and spices. *Food Chem.* **2001**, *73*, 255−261.
(43) Barclay, L. R.; Vinqvist, M. R.; Mukai, K.; Goto, H.; Hashimoto, Y.; Tokunaga, A.; Uno, H. On the antioxidant mechanism of curcumin: Classical methods are needed to determine antioxidant mechanism and activity. *Org. Lett.* **2000**, *2*, 2841−2843.
(44) Cort, W. M. Antioxidant activity of tocopherols, ascorbyl palmitate, and ascorbic acid and their mode of action. *J. Am. Oil Chem. Soc.* **1974**, *51*, 321−325.
(45) Das, K. C.; Das, C. K. Curcumin (diferuloylmethane), a singlet oxygen ($^1O_2$) quencher. *Biochem. Biophys. Res. Commun.* **2002**, *295*, 62−66.
(46) Gutierrez, R. M. P.; Luna, H. H.; Garrido, S. H. Antioxidant activity of *Tagetes erecta* essential oil. *J. Chil. Chem. Soc.* **2006**, *51*, 883−886.
(47) Bhawana.; Basniwal, R. K.; Buttar, H. S.; Jain, V. K.; Jain, N. Curcumin nanoparticles: preparation, characterization, and antimicrobial study. *J. Agric. Food Chem.* **2011**, *59*, 2056−2061.
(48) Litwinienko, G.; Ingold, K. U. Abnormal solvent effects on hydrogen atom abstraction. 2. Resolution of the curcumin antioxidant controversy. The role of sequential proton loss electron transfer. *J. Org. Chem.* **2004**, *69*, 5888−5896.
(49) Weber, W. M.; Hunsaker, L. A.; Abcouwer, S. F.; Deck, L. M.; Vander, Jagt. D. L. Anti-oxidant activities of curcumin and related enones. *Bioorg. Med. Chem.* **2005**, *13*, 3811−3820.
(50) Gordon, M. H. The mechanism of antioxidant action in vitro. In *Food Antioxidants*; Hudson, B. J. F., Ed.; Elsevier: New York, 1990; pp 1−18.
(51) Griffin, S. P.; Bhagooli, R. Measuring antioxidant potential in corals using the FRAP assay. *J. Exp. Mar. Biol. Ecol.* **2004**, *302*, 201−211.
(52) Prior, R. L.; Cao, G. In vivo total antioxidant capacity: comparison of different analytical methods. *Free Radical Biol. Med.* **1999**, *27*, 1173−1181.
(53) Wang, M.; Wu, P.; Sengupta, S. S.; Chadhary, B. I.; Cogen, J. M.; Li, B. Investigation of water diffusion in low-density polyethylene by attenuated total reference Fourier transform infrared spectroscopy and two-dimensional correlation analysis. *Ind. Eng. Chem. Res.* **2011**, *50*, 6447−6454.
(54) Buslov, D. K.; Sushko, N. I.; Tretinnikov, O. N. Study of thermal gelation of methylcellulose in water using FTIR-ATR spectroscopy. *J. Appl. Spectrosc.* **2008**, *75*, 514−518.
(55) Kolev, T. M.; Velcheva, E. A.; Stamboliyska, B. A.; Spiteller, M. DFT and experimental studies of the structure and vibrational spectra of curcumin. *Int. J. Quan. Chem.* **2005**, *102*, 1069−1079.
(56) Bich, V. T.; Thuy, N. T.; Binh, N. T.; Huong, N. T. M.; Yen, P. N. D.; Luong, T. T. Structural and spectral properties of curcumin and metal−curcumin complex derived from turmeric (*Curcuma longa*). Physics and engineering of new materials. *Springer Proc. Phys.* **2009**, *127*, 271−278.
(57) Bratu, I.; Muresan-Pop, M.; Kacso, I.; Fărcaş, I. Spectroscopic investigation of the interaction between β-cyclodextrin and ascorbic acid. *J. Phys. Conf. Ser.* **2009**, *182*, 1−4.